

# UAV Pathfinding in Dynamic Obstacle Avoidance with Multi-agent Reinforcement Learning

Qizhen Wu<sup>1</sup>, Lei Chen<sup>2</sup>, Kexin Liu<sup>3</sup>, Jinhu Lü<sup>4</sup>

**Abstract**—Multi-agent reinforcement learning based methods are significant for online planning of feasible and safe paths for agents in dynamic and uncertain scenarios. Although some methods like fully centralized and fully decentralized methods achieve a certain measure of success, they also encounter problems such as dimension explosion and poor convergence, respectively. In this paper, we propose a novel centralized training with decentralized execution method based on multi-agent reinforcement learning to solve the dynamic obstacle avoidance problem online. In this approach, each agent communicates only with the central planner or only with its neighbors, respectively, to plan feasible and safe paths online. We improve our methods based on the idea of model predictive control to increase the training efficiency and sample utilization of agents. The experimental results in both simulation, indoor, and outdoor environments validate the effectiveness of our method. The video is available at [https://www.bilibili.com/video/BV1gw41197hV/?vd\\_source=9de61aecd9fb684e546d032ef7fe7bf](https://www.bilibili.com/video/BV1gw41197hV/?vd_source=9de61aecd9fb684e546d032ef7fe7bf).

## I. INTRODUCTION

With the development of artificial intelligence, many scholars have found new solutions for the multi-agent pathfinding (MAPF) problem [3], [37], [38], which has many applications [4]–[6] in the actual world. In obstacle avoidance problems, unmanned aerial vehicles (UAVs) should avoid obstacles and collisions between UAVs. The dynamic environment changes in obstacle avoidance bring significant challenges to the traditional MAPF algorithms [35]. However, only the algorithms address the problem of dynamic changes and can be adaptable to the environment for complex tasks.

Reinforcement learning (RL)-based MAPF algorithms show great potential in solving dynamically changing environment problems [8]. As the deep reinforcement learning technique develops, multi-agent reinforcement learning (MRL) algorithms have achieved good results in obstacle avoidance for MAPF. At present, MAPF based on MRL can be categorized by three types [11]: fully centralized [20], fully decentralized [21], and centralized training with decentralized execution [22]. Reference [24], [25], [28], [30] adopt the fully centralized method, which may lead to the dimensional explosion problem. Reference [26], [27], [29], [33],

\*This work was supported by the National Science Foundation of China under Grants 62088101 and 62003015.

<sup>1</sup>Qizhen Wu, <sup>3</sup>Kexin Liu and <sup>4</sup>Jinhu Lü are with the School of Automation Science and Electrical Engineering, Beihang University, Beijing 100191, China. wuqzh7@buaa.edu.cn, skxliu@163.com, jhlu@iss.ac.cn

<sup>2</sup>Lei Chen is with the Advanced Research Institute of Multidisciplinary Sciences, Beijing Institute of Technology, Beijing 100081, China and also with the Yangtze Delta Region Academy of Beijing Institute of Technology, Jiaxing, China. bit\_chen@bit.edu.cn

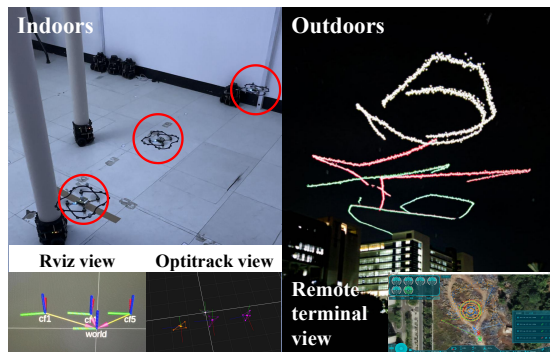


Fig. 1. The scenario of our problem. In this paper, indoor and outdoor experiments are carried out separately. Motion capture cameras and ultra-wide bands are used for UAVs localization indoors and outdoors, respectively.

[34] adopt the fully decentralized method, which happens to cause the non-stationary problem. To enable an agent to eventually learn a decentralized policy that is adaptive to the environment of larger scale agents, Damani [15] combines expert experience to make centralized training. Due to the complexity and variability of the actual environment, as well as the increasing need for scalability and convergence of algorithms, the method of centralized training with decentralized execution will play an increasingly important role in future decision-making problems [12]. Yan [32] applies a centralized training with decentralized execution method of the multi-agent proximal policy optimization to 2D planar obstacle avoidance. Thumiger [25] and Semnani [30] take the obstacle avoidance from 2D to 3D, but only consider in steady state. The algorithms can be more scalable to the environment for complex tasks when they do not depend on expert experience and consider scenarios with dynamic obstacles.

To overcome environmental uncertainty in complex tasks, this paper presents a novel centralized training with decentralized execution method without expert experience for solving dynamic obstacle avoidance problems. First, we propose a centralized training with partially decentralized execution method to address the problems of dimensional explosion and non-stationary for MRL in MAPF. Then, considering the case that the agents are out of contact with the central planner and can communicate with each other, we present a centralized training with fully decentralized execution method so that the agents can make fully decentralized decisions without relying on the central planner. Furthermore, to solve the problem of low training efficiency of MRL in MAPF, we adopt an improved MRL method

based on model predictive control (MPC). It applies a rolling optimization approach to maximize the cumulative return for each prediction interval, which improves the learning efficiency and sample utilization of agents in MARL. The scenario of our problem is shown in Fig.1.

## II. PROBLEM FORMULATION

### A. Decentralized Partially Observable Markov Decision Processes

A fully cooperative multi-agent reinforcement learning task can be described in terms of a decentralized partially observable Markov decision process (Dec-POMDPs). We represent a Markov game for  $I$  agents as a eight-tuple  $(I, S, A, P, r, Z, O, \gamma)$ , where  $s \in S$  denotes the state of the environment.  $a^i \in A$  and  $a \in A \equiv A^I$  denote the action of each agent and the set of joint actions of all agents, respectively.  $P(s'|s, a) : S \times A \rightarrow S$  denotes the state transition function that takes place from state  $s$  to state  $s'$  under the joint actions  $a$ .  $r(s, a) : S \times A \rightarrow R$  denotes the reward function.  $z^i \in Z$  denotes the observation of each agent described by  $O(s, a) : S \rightarrow Z$ .  $z \in Z \equiv Z^I$  denotes the set of joint observations of all agents.  $\gamma \in (0, 1)$  denotes discount factor. The purpose of each agent is to optimize the policy network  $\pi^i$  such that the cumulative reward  $\mathbb{E}_{\Gamma^i \sim \pi^i} [\sum_{t=1}^{\infty} \gamma^t r_t]$ ,  $r_t \sim R^i$  is maximized under the policy.  $\Gamma^i = (s_0^i, a_0^i, s_1^i, a_1^i, \dots)$  is the trajectory of each agent interacting with the environment under the strategy, where  $a_t^i \sim \pi^i(\cdot | z_t^i)$  and  $z_{t+1}^i \sim P(\cdot | z_t^i, a_t^i)$  denote the selected action and reaching observation at each step  $t$ .

### B. Multi-agent Deep Deterministic Policy Gradient

The value function-based RL estimates the optimal state-action value function  $Q^{i*} : O \times A \rightarrow \mathbb{R}$  through a parameterized neural network  $Q_\omega^i(z, a) \approx Q^{i*}(z, a) = \mathbb{E}[R^i(z, a) + \gamma \max_{z', a'} Q^{i*}(z', a')]$ , where  $z', a'$  is the observation and action at the following step.  $\gamma$  denotes the discount factor.  $\omega$  is the weighting factor of the neural network. For  $\gamma \approx 1$ ,  $Q^*$  estimates the discounted returns of the optimal strategy over an infinite range. The multi-agent deep deterministic policy gradient (MADDPG) is based on several fundamental constraints: (a) Each agent can only calculate the action values based on its local observations during the execution of the action; (b) The model is a differential equation that does not take into account the dynamics of the environment; (c) Agents do not consider specific communication protocols or methods with each other. Based on the above constraints, according to the method in Fig.3, MADDPG designs the cost function for each module and calculates the gradient.  $\pi = (\pi^1, \dots, \pi^I)$  and  $\omega = (\omega^1, \dots, \omega^I)$  denote the strategy and critic networks' parameters of  $I$  agents, respectively.  $Q^{i*}$  can be approximated by iteratively fitting  $Q_\omega^i$  and the loss function is described as:

$$L_\omega^i = \mathbb{E}_{(z, a) \sim \mathfrak{B}} \|Q_\omega^i(z, a) - y^i\|^2, \quad (1)$$

where the  $Q$ -target :  $y^i = R^i(z, a) + \gamma \max_{z', a'} Q_\omega^i(z', a')$ .  $\mathfrak{B}$  is a replay buffer that grows iteratively as new data are

collected. The updating rule of  $\omega$  is:

$$\omega_{k+1} \leftarrow \arg \min_{\omega} \mathbb{E}_{(z, a) \sim \mathfrak{B}} \|Q_\omega^i(z, a) - y^i\|^2, \quad (2)$$

where  $\omega^-$  is a slow moving online average. The parameter  $\omega^-$  is updated with the rule  $\omega_{k+1}^- \leftarrow (1 - \zeta)\omega_k^- + \zeta\omega_k$  at each iteration using a constant factor  $\zeta \in [0, 1)$ .  $Q_\omega^i(z, a)$  is a centralized action-value function that takes as input the actions of all agents  $a^1, \dots, a^I$ , in addition to some observation information  $z$ , and outputs the Q-value for agent  $i$ . The detailed description of the MADDPG algorithm can be seen in [13].

### C. UAV 3D Trajectory Constraints

The planned UAV 3D trajectory usually needs to satisfy some basic constraints, including yaw angle, climb angle, trajectory segment length, flight altitude, and total trajectory length. Let  $q_t$  denote the trajectory point in time  $t$ .  $x, w, h$  denote the position in the three directions.  $\theta, \lambda$  denote the yaw and climb angles, respectively. Considering three consecutive trajectory points  $q_{t-1}, q_t, q_{t+1}$ , the 3D trajectory constraints of the UAV can be expressed as follows. The yaw angle constraint refers to the UAV can only turn in the horizontal plane less than or equal to the specified maximum yaw angle:

$$\theta_t = \arccos \frac{(x_{t+1}-x_t)(x_t-x_{t-1})+(w_{t+1}-w_t)(w_t-w_{t-1})}{\sqrt{(x_{t+1}-x_t)^2+(w_{t+1}-w_t)^2} \cdot \sqrt{(x_t-x_{t-1})^2+(w_t-w_{t-1})^2}}, \quad (3)$$

where  $\theta_t \leq \theta_{\max}$  and  $\theta_{\max}$  is the maximum yaw angle. The climb angle constraint, which means the UAV can only climb in the vertical plane less than or equal to the specified maximum climb angle:

$$\lambda_t = \arctan \frac{|h_t-h_{t-1}|}{\sqrt{(x_t-x_{t-1})^2+(w_t-w_{t-1})^2}}, \quad (4)$$

where  $\lambda_t \leq \lambda_{\max}$  and  $\lambda_{\max}$  is the maximum climb angle. The trajectory segment length constraint refers to the shortest range that the UAV can fly in the direction of the current trajectory before it changes the flight attitude:

$$L_t = \sqrt{(x_t-x_{t-1})^2+(w_t-w_{t-1})^2+(h_t-h_{t-1})^2}, \quad (5)$$

where  $L_t \geq L_{\min}$  and  $L_{\min}$  is the minimum trajectory segment length. The flight altitude constraint, which is the safe flight altitude of the UAV:

$$h_{\min} \leq h_t \leq h_{\max}, \quad (6)$$

where  $h_{\max}$  is the maximum altitude and  $h_{\min}$  is the minimum altitude. The total trajectory length constraint, which means the total trajectory length of the UAV is less than or equal to the specified threshold value:

$$\sum_{t=2}^T L_t \leq L_{\max}, \quad (7)$$

where  $L_{\max}$  is the maximum total trajectory length.

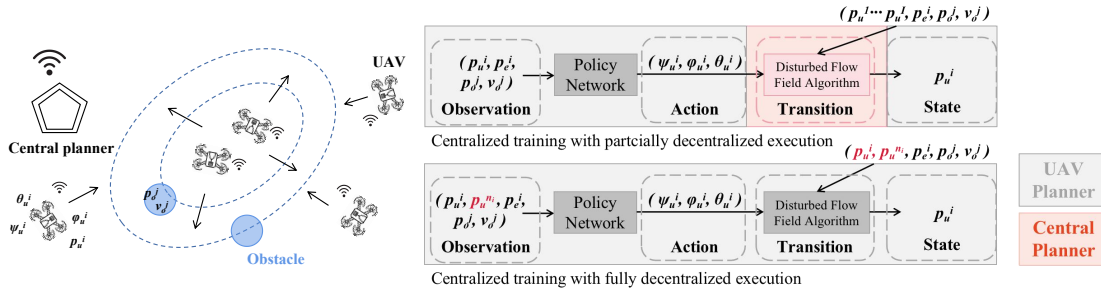


Fig. 2. The MDP of UAV dynamic-obstacle avoidance problem. The left part is the multi-UAV obstacle avoidance scenario. The right part shows the difference between centralized training with partially decentralized execution and centralized training with fully decentralized execution.

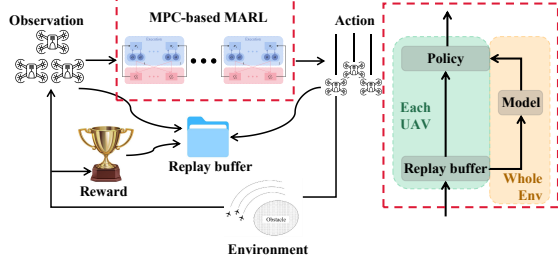


Fig. 3. Framework of MPC-based MARL. The part on the left is the classical interaction model for multi-agent reinforcement learning. We use the samples drawn from the experience replay buffer to update the environment model and each UAV's policy.

### III. MAIN RESULT

Many multi-agent reinforcement learning methods are often limited in swarm tasks by the need for extensive expert experience or lack of consideration of dynamic obstacles. Due to the uncertainty of the environment, designing an online obstacle avoidance method for complex dynamic tasks is crucial for the application of MARL methods. Therefore, we propose a centralized training with partially decentralized execution method in this paper that contains a central planner without expert experience. Considering the constraints of communication, we introduce a centralized training with fully decentralized execution method. The methods provide higher training efficiency and sample utilization via inducing model predictive control.

#### A. Centralized Training with Decentralized Execution Decision Process

Consider the obstacle avoidance problem with  $i$  agents and  $j$  obstacles. Let position and velocity vectors in 3D be denoted by  $p$  and  $v$ , respectively.  $p_u^i, p_o^j, p_e^i$  denote the positions of each UAV center, each obstacle center, and ending point.  $v_o^j$  denotes the velocity of each obstacle.  $\rho_u, \rho_o$  denote the radius of UAVs and obstacles, respectively. The state space  $S$  includes the positions of all UAVs and the positions and speeds of obstacles. To address the problems of dimensional explosion and non-stationary for MARL in MAPF, we propose a centralized training with partially decentralized execution method so that the local observation of the agent contains information about its position information, the end position information, obstacle position information,

and obstacle velocity information. The observation of each UAV for centralized training with partially decentralized execution can be set in the following form:

$$z_t^i = \begin{bmatrix} (p_o^j - p_u^i) \cdot \frac{d_{ou}^{ij} - (\rho_o + \rho_u)}{d_{ou}^{ij}} \\ p_e^i - p_u^i \\ v_o^j \end{bmatrix}. \quad (8)$$

$d_{ou}^{ij} = \|p_o^j - p_u^i\|$  is the distance between the UAV center and obstacle center, where  $\|\cdot\|$  denotes the Euclidean norm. The method mainly considers the case where the central planner can communicate with the agents and does not require the agents to communicate with each other. The algorithm is both adaptable and convergent. To consider the case that the agents are out of contact with the central planner and can communicate with each other, we propose a centralized training with fully decentralized execution method so that the local observation of the agent contains its position information, the end position information, the obstacle position and velocity information, and the neighboring agent position information. The observation of each UAV for centralized training with fully decentralized execution can be set in the following form:

$$z_t^i = \begin{bmatrix} (p_o^j - p_u^i) \cdot \frac{d_{ou}^{i1j} - (\rho_o + \rho_u)}{d_{ou}^{i1j}} \\ p_e^{i1} - p_u^i \\ v_o^j \\ (p_u^{i2} - p_u^{i1}) \cdot \frac{d_{u1u2}^{i1i2} - 2\rho_u}{d_{u1u2}^{i1i2}} \end{bmatrix}. \quad (9)$$

$d_{u1u2}^{i1i2} = \|p_{u1}^{i1} - p_{u2}^{i2}\|$  is the distance between  $i_1$ -th UAV center and  $i_2$ -th UAV center. This method allows the agent to make fully decentralized execution without relying on the central planner. To validate MPC-based MARL in the pathfinding task, we establish the UAV dynamic obstacle avoidance problem as a complete MDP as shown in Fig.2. For centralized training with partially decentralized execution, only the desired heading angle of each UAV needs to be passed to the central planner during the computation of state transition, which in turn outputs the position command for each UAV at the next moment. For centralized training with fully decentralized execution, all processes can be done in each UAV itself by adding local observation information.

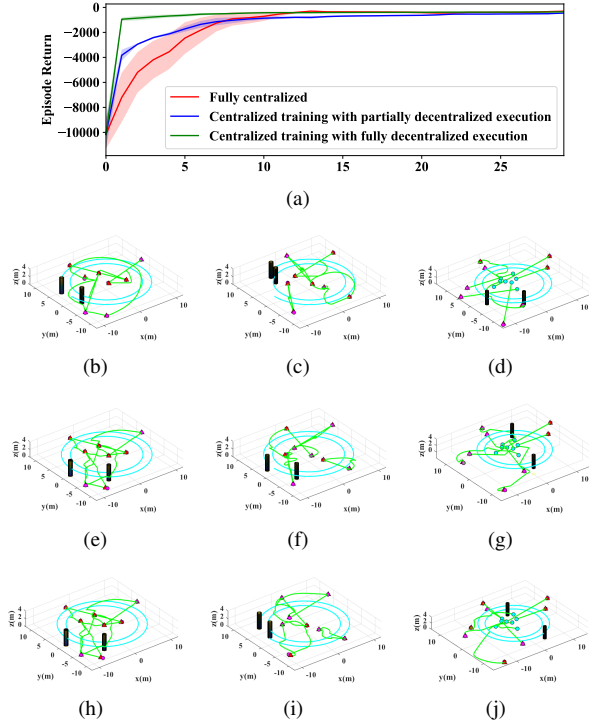


Fig. 4. Comparison with three methods in UAV pathfinding. (a) is the curve of the episode return for three methods. (b)–(d) are validations for fully centralized with different starting and ending points and different task situations, respectively. (e)–(g) are validations for centralized training with partially decentralized execution. (h)–(j) are validation for centralized training with fully decentralized execution.

The action space can be set in the following form:

$$A = [\psi_u^i \quad \theta_u^i \quad \varphi_u^i]^T, \quad (10)$$

where  $\psi_u^i, \theta_u^i, \varphi_u^i$  denote the roll, yaw, and pitch of each UAV, respectively. We design the reward for leading UAVs to avoid dynamic obstacles and achieve shorter pathfinding:

a) If the  $i$ -th UAV collides with the  $j$ -th obstacle ( $d_{ou}^{ij} < \rho_u + \rho_o$ ), there is:

$$r_t = \frac{d_{ou}^{ij} - (\rho_u + \rho_o)}{(\rho_u + \rho_o)} - r_a. \quad (11)$$

b) If the  $i_1$ -th UAV collides with the  $i_2$ -th UAV ( $d_{u_1 u_2}^{i_1 i_2} < 2\rho_u$ ), there is:

$$r_t = \frac{d_{u_1 u_2}^{i_1 i_2} - 2\rho_u}{2\rho_u} - r_a. \quad (12)$$

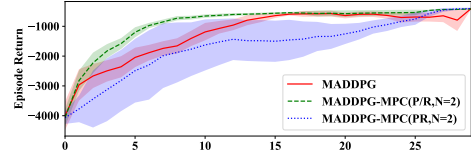
c) Otherwise:

$$r_t = r_{t_1} + r_{t_2} + r_{t_3}, \quad (13)$$

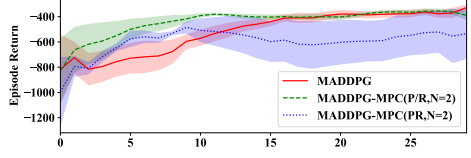
where if the  $i$ -th UAV enters the threat zone of the  $j$ -th obstacle ( $\rho_u + \rho_o < d_{ou}^{ij} < \rho_u + \rho_o + d_{thr}$ ), there is:

$$r_{t_1} = \frac{d_{ou}^{ij} - (\rho_u + \rho_o + d_{thr})}{(\rho_u + \rho_o + d_{thr})} - r_b, \quad (14)$$

otherwise,  $r_{t_1} = 0$ . And if the  $i_1$ -th UAV enters the threat zone of the  $i_2$ -th UAV ( $2\rho_u < d_{u_1 u_2}^{i_1 i_2} < 2\rho_u + d_{thr}$ ), there



(a) Centralized training with partially decentralized execution



(b) Centralized training with fully decentralized execution

Fig. 5. Comparison with baseline in UAV pathfinding. The settings of the parameters are kept the same, except that the buffer size for the MADDPG-MPC method is 10% of MADDPG.

is:

$$r_{t_2} = \frac{d_{u_1 u_2}^{i_1 i_2} - (2\rho_u + d_{thr})}{(2\rho_u + d_{thr})} - r_b, \quad (15)$$

otherwise,  $r_{t_2} = 0$ .

$$r_{t_3} = \begin{cases} -\frac{d_{eu}^i}{d_{es}^i} + r_c & \forall i, d_{eu}^i < d_{com} \\ -\frac{d_{eu}^i}{d_{es}^i} & otherwise \end{cases}, \quad (16)$$

where  $d_{eu}^i = \|p_e^i - p_u^i\|$  denotes the distance between end point and UAV center.  $d_{es}^i = \|p_e^i - p_s^i\|$  denotes the distance between the end point and start points.  $d_{com}$  is a arrival distance, and if  $d_{eu}^i < d_{com}, \forall i$ , the task is completed.  $r_a, r_b$  are constant rewards and  $r_c$  is the additional reward for completing the task.  $d_{thr}$  is a threat distance, and if  $d_{ou} < \rho_u + \rho_o + d_{thr}$ , we consider that UAV is entering the area where it is about to collide with the obstacle. We apply (8)–(13) as the state, action, and reward spaces in the MDP, respectively. In addition, we implement the state transition of the environment  $P(s, a)$  based on the disturbed flow field algorithm [19].

### B. Model Predictive Control-based Multi-agent Deep Deterministic Policy Gradient

The MPC method obtains a local solution to the trajectory optimization problem at each step  $t$  by estimating the optimal action  $a_{t:t+N}$  on a finite horizon  $N$  and executing the first action:

$$u_1^{MPC}(x_t) = \arg \min_{u_{t:t+N}} \mathbb{E} \left[ \sum_{i=t}^{t+N-1} x_i^T G s_i + u_i^T E u_i \right], \quad (17)$$

$$u_2^{MPC}(x_t) = \arg \min_{u_{t:t+N}} \mathbb{E} \left[ \sum_{i=t}^{t+N-1} x_i^T G x_i + u_i^T E u_i + x_N^T P x_N \right], \quad (18)$$

where  $G$ ,  $E$ , and  $P$  are the error weighting matrix, control weighting matrix, and terminal error weighting matrix, respectively. The formula in (17) is the basic MPC, and (18) is the basic MPC with added terminal cost [23].

To solve the problem of low training efficiency of model-free RL, it proposes MPC-based RL method. When combining RL and MPC, we can replace process and terminal costs with rewards and terminal value functions. We unify the notation by replacing  $x$  and  $u$  with the symbols  $z$  and  $a$ , respectively. It obtains the following form by transforming the problem from least cost to most benefit:

$$\pi_1^{MPC}(z_t) = \arg \max_{a_{t:t+N}} \mathbb{E} \left[ \sum_{i=t}^{t+N-1} \gamma^i R(z_i, a_i) \right], \quad (19)$$

$$\pi_2^{MPC}(z_t) = \arg \max_{a_{t:t+N}} \mathbb{E} \left[ \sum_{i=t}^{t+N-1} \gamma^i R(z_i, a_i) + \gamma^N \max Q_{\theta^-}(z_{t+N}, a_{t+N}) \right]. \quad (20)$$

To improve sample utilization of MARL in MAPF, we adopt an improved MARL method based on MPC. It applies a rolling optimization approach to maximize the cumulative return for each prediction interval, which improves the learning efficiency and sample utilization of agents. We replace the reward  $R(z_i, a_i)$  with the return  $\sum_{t=1}^{\infty} \gamma^t r_t$  to maximize both short-term and long-term rewards, and the strategy of each agent can be described in the following form:

$$\pi^{MPC-MARL}(z_t) = \arg \max_{a_{t:t+N}} \mathbb{E} \left[ \sum_{j=t}^N \gamma^j \left( \sum_t^{\infty} \gamma^t r_t \right) \right]. \quad (21)$$

Under (21), we perform predictive control based on a single moment  $t$  to produce a local optimal solution in the present moment. The rolling optimization is then performed to generate multiple locally optimal solutions and calculate the optimal value. By accumulating the returns from the next  $N$  steps in a way that can serve to improve sample utilization and training efficiency. We can also improve the loss function as follows:

$$L_{\omega}^i = \mathbb{E}_{(z_k, a_k) \sim \mathfrak{B}} \sum_{n=0}^{N-1} \|Q_{\omega}^i(z_{k+n}, a_{k+n}) - y_{k+n}^i\|^2, \quad (22)$$

where the  $Q$ -target is modified as follows:

$$y_{k+n}^i = \sum_{j=n}^{N-1} \gamma^j R(z_{k+i}, a_{k+i}) + \gamma^N \max Q_{\omega^-}^i(z_{k+N}, a_{k+N}). \quad (23)$$

Similarly, we can improve the updating rule of  $\omega$  as follows:

$$\omega_{k+1}^i \leftarrow \arg \min_{\omega} \mathbb{E}_{(z_k, a_k) \sim \mathfrak{B}} \left\{ \sum_{n=0}^{N-1} \|Q_{\omega}^i(z_{k+n}, a_{k+n}) - y_{k+n}^i\|^2 \right\}. \quad (24)$$

The flowchart of our MPC-based MADDPG approach is shown in Algorithm 1. The framework of MPC-based MARL is shown in Fig.3. We build neural networks with

states transition function  $P_{\theta}$  and reward function  $R_{\tau}$  to model the environment. We use the samples drawn from the experience replay buffer to update the environment model and each UAV's policy. Meanwhile, the environment model has a facilitating effect on the update of the policy model of each UAV. Next, we can verify the performance of MPC-based MARL based on this MDP model and conduct validation experiments in simulated and realistic environments.

---

#### Algorithm 1 MPC-based MADDPG

---

**Input:** Discount factor( $\gamma$ ); Learning rate( $\alpha$ );  
Training episode( $E$ ); Training step( $T$ );  
Stochastic noise( $\mathfrak{N}$ ); Prediction step( $N$ );

**Output:** Policy-network( $\pi_{\beta}^i$ )

- 1: Initialize networks  $\omega^i, \beta^i, \theta, \tau$  and the replay buffer  $\mathfrak{B}$ ;
- 2: **for all**  $e = 1 \rightarrow E$  **do**
- 3:   Get the initial observation  $z_0$ ;
- 4:   **for all**  $t = 1 \rightarrow T$  **do**
- 5:     Use the strategy  $\pi_{\beta}^i(z)$  and noise  $\mathfrak{N}$  to select  $a_t^i$  in the current observation  $z_t$ ,  $a_t = (a_t^1, \dots, a_t^I)$ ;
- 6:      $r_t, z_{t+1} \leftarrow Env$
- 7:      $\mathfrak{B} \leftarrow (z_t, a_t, r_t, z_{t+1})$ ;
- 8:     **for all**  $i = 1 \rightarrow I$  **do**
- 9:        $(z_k^i, a_k^i, r_k, z_{k+1}^i)_{k=1, \dots, K} \leftarrow \mathfrak{B}$ ;
- 10:       **if**  $L_{\theta} < \epsilon_l^{\theta}$  and  $L_{\tau} < \epsilon_l^{\tau}$  **then**
- 11:         **for all**  $n = 0 \rightarrow N$  **do**
- 12:         Use the strategy  $\pi_{\beta}^i(z)$  and noise  $\mathfrak{N}$  to select  $a_{k+n}^i$  in the current observation  $z_{k+n}$ ;
- 13:          $z_{k+n+1}^{\theta}, r_{k+n}^{\tau} \leftarrow P_{\theta}(z, a), R_{\tau}(z, a)$ ;
- 14:          $y_{k+n}^i \leftarrow \sum_{j=n}^{N-1} \gamma^j r_{k+j}^{\tau} + \gamma^N Q_{\omega^-}^i(z_{k+N}^{\theta}, a_{k+N})$ ;
- 15:          $L_{\omega}^i = \frac{1}{K} \sum_k \left\{ \sum_n [y_{k+n}^i - Q_{\omega}^i(z_{k+n}^{\theta}, a_{k+n})]^2 \right\}$ ;
- 16:         **end for**
- 17:       **else**
- 18:         Use the strategy  $\pi_{\beta}^i(z)$  and noise  $\mathfrak{N}$  to select  $a_{k+1}^i$  in the current observation  $z_{k+1}$ ;
- 19:          $y_k^i \leftarrow r_k + \gamma Q_{\omega}^i(z_k, a_k)$ ;
- 20:          $L_{\omega}^i = \frac{1}{K} \sum_k \left\{ \sum_n [y_k^i - Q_{\omega}^i(z_k, a_k)]^2 \right\}$ ;
- 21:       **end if**
- 22:     **end for**
- 23:      $L_{\theta} = \frac{1}{K} \sum_k (z_{k+1}^{\theta} - z_{k+1})^2$ ;
- 24:      $L_{\tau} = \frac{1}{K} \sum_k (r_k^{\tau} - r_k)^2$ ;
- 25:     Refresh networks  $\omega^i, \beta^i, \theta, \tau$ ;
- 26:   **end for**
- 27: **end for**

---

## IV. EXPERIMENTS

In this section, we adopt MADDPG [13] as the baseline and compare the partially decentralized execution and fully decentralized execution in UAV pathfinding in Fig.4. We evaluate our proposed MPC-based MADDPG and compare

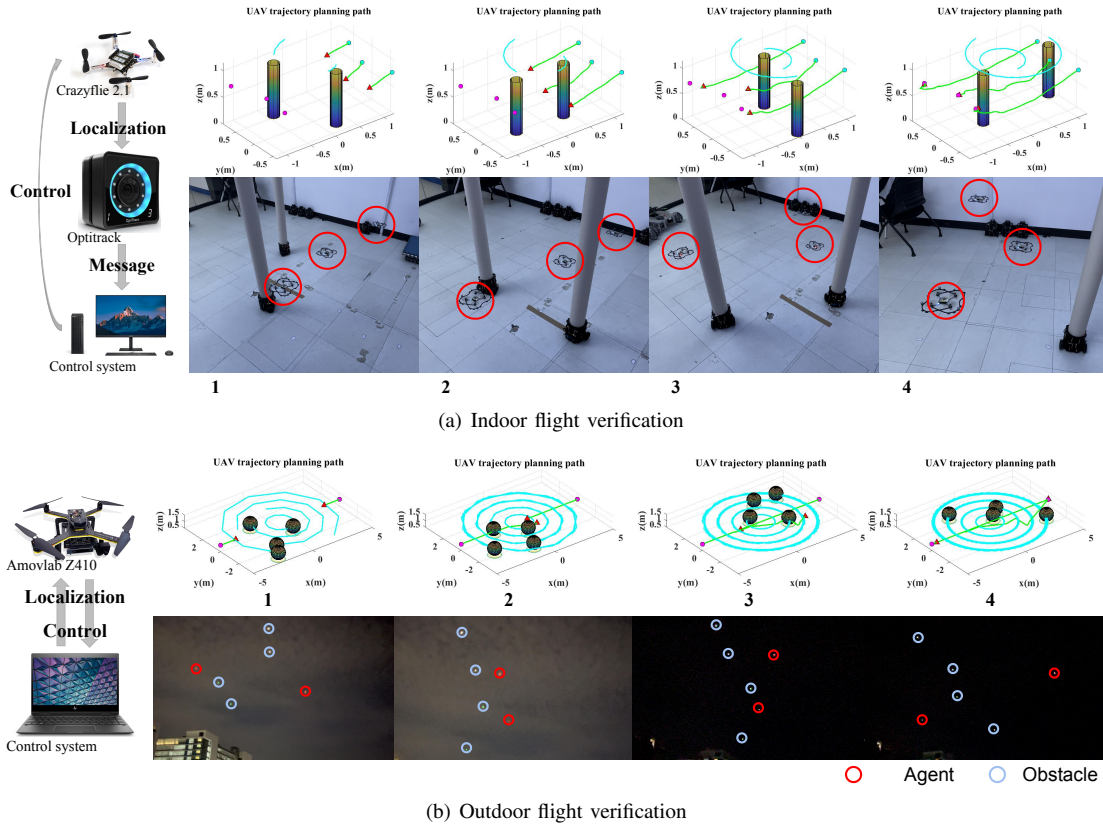


Fig. 6. Flight verification. We validate the algorithm indoors and outdoors, respectively. In each of the eight sets of plots in (a) and (b), the top four plots show the actual trajectories of the UAVs, and the bottom four plots show the actual flight scenes.

its performance against baselines on the designed UAV dynamic obstacle avoidance environment in Fig.5.

For both three methods, UAVs have the same initial return. However, centralized training with fully decentralized execution method is the fastest convergence to the optimal value. With continuous training, the returns of the three methods gradually become the same. This result illustrates that centralized training with fully decentralized execution method is optimal, while centralized training with partially decentralized execution method is inferior. We obtain better results in both modes by modeling the P-network and R-network into two separate neural networks. The buffer size of MADDPG-MPC is 10% of MADDPG, but it can significantly reduce the number of sample interactions required for the strategy to converge to the optimal value. Through comparisons, MADDPG-MPC leads the strategy to quickly converge to the optimal value based on fewer interaction data and frees up more sample capacity space required for the experience replay buffer.

In order to verify the feasibility of the designed centralized training with fully decentralized execution approach, we conduct experiments with a actual UAV swarm. In the actual UAV experiments, we adopt the method of simulation to reality [36]. We simulate the obstacle avoidance scenarios in the actual mission through the simulation environment, including the dynamics of the UAVs, the movement of the obstacles, and the target position of the UAVs. In an indoor

experiment as shown in Fig.6a, we use two plastic tubes with a radius of 0.1 meters and a height of 1 meter as cylindrical obstacles, and three UAVs traverse the obstacles from one end to the other. This scenario is similar to the actual-life UAV swarm avoiding moving crowds. In an outdoor experiment as shown in Fig.6b, we use four UAVs with a radius of about 0.2 meters as orb obstacles, and two UAVs traverse the obstacles from each end to each other. By performing MPC-based MADDPG training in the simulation environment, we can get the policy network of UAV swarm in this scenario. Based on this strategy network, the UAV swarm can avoid obstacles well in the actual mission scenario and reach the target position while ensuring they will not collide. The success of the experiments verifies that the centralized training with fully decentralized execution method we designed can accomplish the UAV swarm obstacle avoidance task by offline training and online decision-making, and this MARL method is improved based on MPC.

## V. CONCLUSIONS

This paper has presented a novel centralized training with decentralized execution method based on UAV swarm obstacle avoidance tasks. By evolving from partially decentralized execution to fully decentralized execution, we have addressed the constraint of communication. With this approach, UAVs have completed the obstacle avoidance task

without relying on the central planner and only based on their local observation. We have proposed the MPC-based MADDPG method to improve agents' learning efficiency and sample utilization in MARL.

## REFERENCES

- [1] R. Barták, J. Švancara, V. Škopková, and D. Nohejl, "Multi-agent path finding on real robots: First experience with ozobots," in *2018 Proc. Adv. Artif. Intell.* Springer, 2018, pp. 290–301.
- [2] L. Cohen, G. Wagner, D. Chan, H. Choset, N. Sturtevant, S. Koenig, and T. Kumar, "Rapid randomized restarts for multi-agent path finding solvers," in *2018 Proceedings of the International Symposium on Combinatorial Search (SOCS)*, vol. 9, no. 1, 2018, pp. 148–152.
- [3] H. Ma, D. Harabor, P. J. Stuckey, J. Li, and S. Koenig, "Searching with consistent prioritization for multi-agent path finding," in *2019 Proc. AAAI Conf. Artif. Intell. (AAAI)*, vol. 33, no. 01, 2019, pp. 7643–7650.
- [4] J. Cartucho, R. Ventura, and M. Veloso, "Robust object recognition through symbiotic deep learning in mobile robots," in *2018 Proc. Int. Conf. Intell. Robots Syst. (IROS)*. IEEE, 2018, pp. 2336–2341.
- [5] S. Choudhury, K. Solovey, M. Kochenderfer, and M. Pavone, "Co-ordinated multi-agent pathfinding for drones and trucks over road networks," in *2022 Proc. Auton. Agent. Multi. Agent Syst. (AAMAS)*, no. 09, 2022, pp. 272–280.
- [6] J. Li, A. Tinka, S. Kiesel, J. W. Durham, T. S. Kumar, and S. Koenig, "Lifelong multi-agent path finding in large-scale warehouses," in *2021 Proc. AAAI Conf. Artif. Intell. (AAAI)*, vol. 35, no. 13, 2021, pp. 11 272–11 281.
- [7] R. Stern, N. Sturtevant, A. Felner, S. Koenig, H. Ma, T. Walker, J. Li, D. Atzmon, L. Cohen, T. Kumar *et al.*, "Multi-agent pathfinding: Definitions, variants, and benchmarks," in *2019 Proceedings of the International Symposium on Combinatorial Search (SOCS)*, vol. 10, no. 1, 2019, pp. 151–158.
- [8] R. Stern, "Multi-agent path finding—an overview," *Artif. Intell.*, pp. 96–115, Oct. 2019.
- [9] R. S. Sutton and A. G. Barto, *Reinforcement learning: An introduction*. MIT press, 2018.
- [10] Q. Liu, L. Shi, L. Sun, J. Li, M. Ding, and F. Shu, "Path planning for uav-mounted mobile edge computing with deep reinforcement learning," *IEEE Trans. Veh. Technol.*, vol. 69, no. 5, pp. 5723–5728, May 2020.
- [11] L. Dong, Z. He, C. Song, and C. Sun, "A review of mobile robot motion planning methods: from classical motion planning workflows to reinforcement learning-based architectures," *J. Syst. Eng. Electron.*, vol. 34, no. 2, pp. 439–459, Apr. 2023.
- [12] P. Hernandez-Leal, B. Kartal, and M. E. Taylor, "A survey and critique of multiagent deep reinforcement learning," *Auton. Agents Multi-Agent Syst.*, vol. 33, no. 6, pp. 750–797, Oct. 2019.
- [13] R. Lowe, Y. I. Wu, A. Tamar, J. Harb, O. Pieter Abbeel, and I. Mordatch, "Multi-agent actor-critic for mixed cooperative-competitive environments," *Adv. Neural Inf. Process. Syst.*, vol. 30, Dec. 2017.
- [14] J. Foerster, G. Farquhar, T. Afouras, N. Nardelli, and S. Whiteson, "Counterfactual multi-agent policy gradients," in *2018 Proc. AAAI Conf. Artif. Intell. (AAAI)*, vol. 32, no. 1, 2018.
- [15] M. Damani, Z. Luo, E. Wenzel, and G. Sartoretti, "Primal\_2: Pathfinding via reinforcement and imitation multi-agent learning-lifelong," *IEEE Rob. Autom. Lett.*, vol. 6, no. 2, pp. 2666–2673, Apr. 2021.
- [16] B. Riviere, W. Hönig, Y. Yue, and S.-J. Chung, "Glas: Global-to-local safe autonomy synthesis for multi-robot motion planning with end-to-end learning," *IEEE Rob. Autom. Lett.*, vol. 5, no. 3, pp. 4249–4256, 2020.
- [17] Q. Li, F. Gama, A. Ribeiro, and A. Prorok, "Graph neural networks for decentralized multi-robot path planning," in *2020 Proc. Int. Conf. Intell. Robots Syst. (IROS)*. IEEE, 2020, pp. 11 785–11 792.
- [18] Y.-b. Chen, G.-c. Luo, Y.-s. Mei, J.-q. Yu, and X.-l. Su, "Uav path planning using artificial potential field method updated by optimal control theory," *Int. J. Syst. Sci.*, vol. 47, no. 6, pp. 1407–1420, 2016.
- [19] P. Yao, H. Wang, and Z. Su, "Uav feasible path planning based on disturbed fluid and trajectory propagation," *Chinese J. Aeronaut.*, vol. 28, no. 4, pp. 1163–1177, June 2015.
- [20] C. Sun, W. Liu, and L. Dong, "Reinforcement learning with task decomposition for cooperative multiagent systems," *IEEE Trans. Neural Networks Learn. Syst.*, vol. 32, no. 5, pp. 2054–2065, May 2020.
- [21] K. Sivanathan, B. Vinayagam, T. Samak, and C. Samak, "Decentralized motion planning for multi-robot navigation using deep reinforcement learning," in *2020 Proceedings of the International Conference on Intelligent Sustainable Systems (ICISS)*. IEEE, 2020, pp. 709–716.
- [22] A. Tampuu, T. Matiisen, D. Kodelja, I. Kuzovkin, K. Korjus, J. Aru, J. Aru, and R. Vicente, "Multiagent cooperation and competition with deep reinforcement learning," *PLoS ONE*, vol. 12, no. 4, p. e0172395, Apr. 2017.
- [23] C. E. Garcia, D. M. Prett, and M. Morari, "Model predictive control: Theory and practice—a survey," *Automatica*, vol. 25, no. 3, pp. 335–348, May 1989.
- [24] Z. Pu, T. Zhang, X. Ai, T. Qiu, and J. Yi, "A deep reinforcement learning approach combined with model-based paradigms for multi-agent formation control with collision avoidance," *IEEE Trans. Syst. Man Cybern.: Syst.*, vol. 53, no. 7, pp. 4189–4204, July 2023.
- [25] N. Thumiger and M. Deghat, "A multi-agent deep reinforcement learning approach for practical decentralized uav collision avoidance," *IEEE Control Syst. Lett.*, vol. 6, pp. 2174–2179, Dec. 2021.
- [26] Y. F. Chen, M. Liu, M. Everett, and J. P. How, "Decentralized non-communicating multiagent collision avoidance with deep reinforcement learning," in *2017 Proc. Int. Conf. Robot. Autom. (ICRA)*. IEEE, 2017, pp. 285–292.
- [27] T. Fan, P. Long, W. Liu, and J. Pan, "Distributed multi-robot collision avoidance via deep reinforcement learning for navigation in complex scenarios," *Int. J. Robot. Res.*, vol. 39, no. 7, pp. 856–892, May 2020.
- [28] W. Ding, S. Li, H. Qian, and Y. Chen, "Hierarchical reinforcement learning framework towards multi-agent navigation," in *2018 Proceedings of the International Conference on Robotics and Biomimetics (ROBIO)*. IEEE, 2018, pp. 237–242.
- [29] Z. Liu, B. Chen, H. Zhou, G. Koushik, M. Hebert, and D. Zhao, "Mapper: Multi-agent path planning with evolutionary reinforcement learning in mixed dynamic environments," in *2020 Proc. Int. Conf. Intell. Robots Syst. (IROS)*. IEEE, 2020, pp. 11 748–11 754.
- [30] S. H. Semmani, H. Liu, M. Everett, A. De Ruiter, and J. P. How, "Multi-agent motion planning for dense and dynamic environments via deep reinforcement learning," *IEEE Rob. Autom. Lett.*, vol. 5, no. 2, pp. 3221–3226, Feb. 2020.
- [31] G. Sartoretti, J. Kerr, Y. Shi, G. Wagner, T. S. Kumar, S. Koenig, and H. Choset, "Primal: Pathfinding via reinforcement and imitation multi-agent learning," *IEEE Rob. Autom. Lett.*, vol. 4, no. 3, pp. 2378–2385, Mar. 2019.
- [32] Y. Yan, X. Li, X. Qiu, J. Qiu, J. Wang, Y. Wang, and Y. Shen, "Relative distributed formation and obstacle avoidance with multi-agent reinforcement learning," in *2022 Proc. Int. Conf. Robot. Autom. (ICRA)*. IEEE, 2022, pp. 1661–1667.
- [33] Y. F. Chen, M. Everett, M. Liu, and J. P. How, "Socially aware motion planning with deep reinforcement learning," in *2017 Int. Conf. Intell. Robots Syst. (IROS)*. IEEE, 2017, pp. 1343–1350.
- [34] P. Long, T. Fan, X. Liao, W. Liu, H. Zhang, and J. Pan, "Towards optimally decentralized multi-robot collision avoidance via deep reinforcement learning," in *2018 IEEE Int. Conf. Robot. Autom. (ICRA)*. IEEE, 2018, pp. 6252–6259.
- [35] T. Huang, J. Li, S. Koenig, and B. Dilkina, "Anytime multi-agent path finding via machine learning-guided large neighborhood search," in *2022 Proc. AAAI Conf. Artif. Intell. (AAAI)*, vol. 36, no. 9, 2022, pp. 9368–9376.
- [36] W. Zhao, J. P. Queralta, and T. Westerlund, "Sim-to-real transfer in deep reinforcement learning for robotics: a survey," in *2020 Proceedings of Symposium Series on Computational Intelligence (SSCI)*. IEEE, 2020, pp. 737–744.
- [37] X. Zhong, J. Li, S. Koenig, and H. Ma, "Optimal and bounded-suboptimal multi-goal task assignment and path finding," in *2022 IEEE Int. Conf. Robot. Autom. (ICRA)*. IEEE, 2022, pp. 10 731–10 737.
- [38] J. Kottinger, S. Almagor, and M. Lahijanian, "Maps-x: Explainable multi-robot motion planning via segmentation," in *2021 IEEE Int. Conf. Robot. Autom. (ICRA)*. IEEE, 2021, pp. 7994–8000.